Ann Allergy Asthma Immunol 121 (2018) 200–210

Contents lists available at ScienceDirect

Aspergillus fumigatus viability drives allergic responses to inhaled conidia

Ajay P. Nayak, PhD [*]; Tara L. Croston, PhD [*]; Angela R. Lemons, MS [*]; W.T. Goldsmith, BS [*]; Nikki B. Marshall, PhD [*]; Michael L. Kashon, PhD [*]; Dori R. Germolec, PhD [†]; Donald H. Beezhold, PhD [*]; Brett J. Green, PhD [*]

[*] *Health Effects Laboratory Division, National Institute for Occupational Safety and Health, Centers for Disease Control and Prevention, Morgantown, West Virginia*
[†] *Toxicology Branch, Division of National Toxicology Program, National Institute of Environmental Health Sciences, Research Triangle Park, North Carolina*

ARTICLE INFO

Article history:
Received for publication February 12, 2018.
Received in revised form April 3, 2018.
Accepted for publication April 9, 2018.

ABSTRACT

Background: *Aspergillus fumigatus*–induced allergic airway disease has been shown to involve conidial germination in vivo, but the immunological mechanisms remain uncharacterized.
Objective: A subchronic murine exposure model was used to examine the immunological mediators that are regulated in response to either culturable or nonculturable *A fumigatus* conidia.
Methods: Female B6C3F1/N mice were repeatedly dosed via inhalation with 1×105 viable or heat-inactivated conidia (HIC), twice per week for 13 weeks (26 exposures). Control mice inhaled high-efficiency particulate arrestor–filtered air. The influence of *A fumigatus* conidial germination on the pulmonary immunopathological outcomes was evaluated by flow cytometry analysis of cellular infiltration in the airways, assessment of lung messenger RNA expression, quantitative proteomics, and histopathology of whole lung tissue.
Results: Repeated inhalation of viable conidia, but not HIC, resulted in allergic inflammation marked by vascular remodeling, extensive eosinophilia, and accumulation of alternatively activated macrophages (AAMs) in the murine airways. More specifically, mice that inhaled viable conidia resulted in a mixed TH1 and TH2 (IL-13) cytokine response. Recruitment of eosinophils corresponded with increased Ccl11 transcripts. Furthermore, genes associated with M2 or alternatively activated macrophage polarization (eg, Arg1, Chil3, and Retnla) were significantly up-regulated in viable *A fumigatus*–exposed mice. In mice inhaling HIC, CD4+ T cells expressing IFN-γ (TH1) dominated the lymphocytic infiltration. Quantitative proteomics of the lung revealed metabolic reprogramming accompanied by mitochondrial dysfunction and endoplasmic reticulum stress stimulated by oxidative stress from repetitive microbial insult.
Conclusion: Our studies demonstrate that *A fumigatus* conidial viability in vivo is critical to the immunopathological presentation of chronic fungal allergic disease.
Published by Elsevier Inc. on behalf of the American College of Allergy, Asthma & Immunology.

Introduction

The distribution of aerosolized conidia can be significantly higher in contaminated indoor (>10^4 spores/m^3) and occupational environments (>10^6 spores/m^3) and can induce diverse health problems.[1,2] To date, the effect of chronic antigenic stimulation from inhaled viable *Aspergillus fumigatus* spores on the development of allergic airway disease has remained inadequately characterized.

In situ germination of *A fumigatus* can have negative clinical consequences in immunocompromised individuals; however, the effect of germination on allergic airway disease is unclear. Exposure to viable *A fumigatus* conidia has been shown to promote T_H1 (proinflammatory) responses, whereas heat-inactivated conidia (HIC) drive expansion of T_H2 (allergic) responses marked by increased expression of interleukin (IL)-13.[3] In a previous study conducted in our laboratory, repeated instillation of HIC *A fumigatus* suspension resulted in accumulation of eosinophils in the airways of mice.[4] Collectively, these studies indicate that exposure to HIC promotes allergic responses in the lungs. However, molecular analyses have indicated that fungal allergens typically include proteases that are associated with germination and hyphal development.[5,6] Fungal spore germination also has been established as a critical step for the

Reprints: Ajay P. Nayak, PhD, Center for Translational Medicine, Department of Medicine, Thomas Jefferson University, 1020 Locust Street, Philadelphia, PA 19107; E-mail: Ajay.Nayak@jefferson.edu.
Disclosures: The authors have no conflict(s) of interest to declare.
Funding Sources: This study was funded by CDC/NIOSH funding 927ZLCT to AN, and in part by an interagency agreement between CDC/NIOSH and National Institute of Environmental Health Sciences (NIEHS) (AES12007001-1-0-6) as a collaborative National Toxicology Program (NTP) research activity.

https://doi.org/10.1016/j.anai.2018.04.008
1081-1206/Published by Elsevier Inc. on behalf of the American College of Allergy, Asthma & Immunology.

expression of some allergens recognized by immunoglobulin E (IgE) from sensitized patients.[6]

Aspergillus fumigatus conidia are capable of persisting in host cells by directly inhibiting phagocytosis.[7] Germinating *A fumigatus* conidia are frequently observed in alveolar macrophages.[8–10] More recently, our laboratory highlighted the differential transcriptional regulation in murine lungs after inhalation of viable and HIC *A fumigatus*.[11] More specifically, we reported down-regulation of specific microRNAs involved in the regulation of pro-allergic cytokines IL-33 and IL-13 in response to inhalation of viable *A fumigatus*.

Repeated inhalation of fungi can cause damage to the host tissue and interfere with the fungal clearance and consequently aid fungal persistence and germination of the deposited conidia. We sought to define the role of conidial viability in the development of allergic immune responses, using our mouse model of repeated inhalation of *A fumigatus*. Furthermore, the immunopathological outcomes of inhaling HIC were compared to viable conidia from *A fumigatus* to identify the critical immunopathological networks that are activated as a result of chronic exposure to fungal aerosols.

Methods

Fungal Cultures, Animals, and Aerosol Exposures

Aspergillus fumigatus B5233 strain was cultured on rice, using previously described methods.[10] Heat-inactivated conidia were generated by autoclaving *A fumigatus* cultures at 121°C for 15 minutes. Viability was assessed by plating serial dilutions of autoclaved or untreated conidia on Malt Extract Agar medium and colony-forming units (cfu/mL) quantified at 72 hours.

Female B6C3F1/N mice (5–6 weeks old) were obtained from NTP/Taconic (Germantown, New York). Acclimatization and exposure of animals were conducted as previously described.[8,10] All animal procedures were approved by the National Institute for Occupational Safety and Health (NIOSH) Animal Care and Use Committee. B6C3F1/N mice were exposed to high-efficiency particulate arrestor–filtered air, aerosolized viable conidia, or HIC (1×10^5 per animal per exposure), twice per week for 13 weeks, using the Acoustical Generator System (AGS) and a nose-only exposure chamber as previously described.[10] At 24 and 48 hours after the final exposure, mice were killed.

Tissue Preparation, Flow Cytometry Staining, and Differential Analysis

After collection of bronchoalveolar lavage fluid (BALF),[10] cell suspensions from lungs were generated, enumerated, and stained with fluorochrome-conjugated antibodies described previously, using previously described methods.[12] For intracellular cytokine staining, a fraction of BALF cells were treated with leukocyte activation cocktail containing GolgiPlug (BD Bioscience, San Jose, California). After staining for surface markers, cells were permeabilized and stained for intracellular cytokines. To minimize nonspecific binding, cells were incubated with Fc Block (BD Bioscience) and rat serum before staining.

Microscopy and Histopathological Assessment

Aspergillus fumigatus conidia were collected from the AGS and processed for field emission scanning electron microscopy.[9] Paraffin-embedded lung tissue sections were stained with hematoxylin and eosin, Grocott's methenamine stain (GMS), Masson's trichrome stain, or alcian blue/periodic acid-Schiff stain to assess histopathological changes. Sections were analyzed using an Olympus AX70 microscope (Olympus America Inc, Center Valley, Pennsylvania) interfaced to an Olympus DP73 camera. All images were acquired and processed using the CELLSENS imaging software (Olympus America Inc)

Sodium Dodecyl Sulfate Polyacrylamide Gel Electrophoresis, Western Blot Analysis, and Enzyme-Linked Immunosorbent Assays

For sodium dodecyl sulfate polyacrylamide gel electrophoresis (SDS-PAGE) and western blot analysis, protein extracts were generated from viable *A fumigatus* and HIC by harvesting cultures grown on rice using sterile dH_2O, frozen at -80°C, and processed by bead beating. Proteins were extracted in sterile phosphate-buffered saline. For western blot analysis, conidial extract derived from viable conidia and HIC was resolved by SDS-PAGE and transferred onto a nitrocellulose membrane. The membrane was blocked with Tris-buffered saline containing 0.05% Tween-20 and 3% dry nonfat dry milk powder, then incubated with pooled serum obtained from mice repeatedly dosed with *A fumigatus* (*Δalb1*) conidia and developed using methods previously described[8] using 1-Step nitro-blue tetrazolium and 5-bromo-4-chloro-3'-indolyphosphate developing solution (Thermo Fisher Scientific, Waltham, Massachusetts).

Enzyme-linked immunosorbent assay (ELISA) for IgG isotypes was performed using methods described previously.[10] The IgE titers were determined using the ELISA MAX mouse IgE kit as per manufacturer's instructions (BioLegend, San Diego, California).

Messenger RNA Expression Analysis

Murine lungs (n = 3 mice/group) were harvested from mice after exposure. Total RNA was isolated from whole lung homogenate using Qiagen's RNeasy Plus Universal RNA Isolation Kit, following the manufacturer's protocol (Qiagen, Stanford, California).

For array, complementary DNA (cDNA) was generated by the RT^2 First Strand Kit according to manufacturer's instructions (Qiagen, California). Equal amounts of cDNA were added to prefabricated plates that included primers to genes grouped into the Th1-Th2 response (RT^2 Profiler PCR Array Mouse Th1 & Th2 Responses; Qiagen, California). The polymerase chain reaction (PCR) plates were subjected to real-time PCR using RT^2 SYBR Green ROX qPCR Mastermix for quantification of cDNA (Qiagen, California). Data were normalized to *Gapdh* and the relative expression of Th1-Th2 genes was analyzed.

Total RNA was also converted to cDNA using the High Capacity cDNA Reverse Transcription Kit with RNase Inhibitor (Life Technologies, Massachusetts). Equal amounts of cDNA were subjected to real-time qPCR measuring additional genes (reported in Table 1). TaqMan Fast Universal PCR Master Mix (2×), no AmpErase UNG (Life Technologies) was used for qPCR reactions. Data were normalized to *Gapdh*, and relative expression is presented with fold change calculated using the delta delta cycle threshold (ΔΔCT) method.

Quantitative Proteomics Analysis

Murine lungs were harvested and digested to obtain protein extracts. Proteins were separated using an SDS-PAGE gel followed by in-gel digestion with trypsin. Digested peptides were analyzed by nano-liquid chromatography tandem mass spectrometry by MS Bioworks (Ann Arbor, Michigan) using a Waters NanoAcquity high-pressure liquid chromatography system interfaced with an Orbitrap Velos Mass Spectrometer. Peptide ion data were searched against the *Mus musculus* genome database (SwissProt). For label-free quantification, data were searched with the following parameters: enzyme—trypsin; fixed modification—carbamidomethyl; variable modifications—Oxidation, Acetyl, Deamidation, Pyro-Glu; peptide mass tolerance—10 ppm. Data were filtered at less than 1% protein false discovery rate. Quantification was performed by spectral count (SpC) analysis, in which spectral numbers of peptides were assigned to each protein from Scaffold software for validation, filtering, and to create a nonredundant list for each sample. These data were analyzed by normalized spectral abundance factor (NSAF) method

Table 1
Whole-Lung mRNA Expression Profiles

Gene		Exposure group comparisons											
		Viable vs control		HIC vs control		Viable vs HIC		Viable vs control		HIC vs control		Viable vs HIC	
Locus	Description	24 hours						48 hours					
		Fold change	*P* value	Fold change	*P* value	Fold change	*P* value	Fold change	*P* value	Fold change	*P* value	Fold change	*P* value
Arg1	Arginase 1	4.57	.2078	–1.61	.6837	7.37	.0905	**22.60**	**.0103**	1.73	.2473	**13.04**	**.0110**
Ccl5*	RANTES	–1.42	.4224	–1.05	.7032	–1.24	.4642	1.44	.4488	1.08	.8813	1.33	.5773
Ccl7*	MCP-3	5.77	.9243	2.49	.3934	–1.23	.3736	21.58	.2589	2.28	.1600	9.45	.2755
Ccl11*	Eotaxin-1	**12.28**	**.0006**	2.16	.2097	**4.64**	**.0042**	**11.56**	**.0074**	1.11	.7690	**10.41**	**.0074**
Cd163	Scavenger receptor type I	–2.99	.0940	–1.94	.2665	–1.55	.0733	1.54	.8317	2.74	.1633	–1.78	.5166
Cd209a	DC-SIGN	–1.64	.5419	–2.20	.3635	1.35	.4979	2.30	.1747	1.58	.5882	1.45	.6424
Chil3	Chitinase-like 3	12.00	.0730	–2.44	.3082	**29.24**	**.0159**	**36.42**	**.0007**	1.43	.6873	**25.40**	**.0122**
Clec4e	MINCLE	1.59	.6210	1.22	.8481	1.30	.7137	**5.06**	**.0040**	5.42	.2697	–1.07	.9603
Clec4n	Dectin-2	1.02	.9811	–1.93	.5120	1.98	.3095	2.35	.1575	2.17	.4299	1.08	.9201
Clec7a	Dectin-1	**4.51**	**.0326**	–1.10	.8071	**4.98**	**.0500**	6.16	.0591	1.42	.5662	**4.34**	**.0208**
Gata3	GATA binding protein 3	**–3.25**	**.0013**	4.69	.3405	**–3.97**	**.0249**	–3.16	.0717	–1.38	.5516	–2.29	.1540
Il1rl1*	Interleukin 1 receptor-like 1 (ST2)	1.29	.7934	–1.12	.6667	–1.02	.7312	**5.91**	**.0267**	1.90	.3697	**3.11**	**.0378**
Il4*	Interleukin 4	1.63	.6480	–1.32	.9809	–1.33	.4986	3.34	.2366	–1.39	.4060	4.64	.2032
Il6*	Interleukin 6	2.24	.5486	1.43	.1735	–2.09	.1953	**13.14**	**.0465**	1.53	.6023	8.61	.0536
Il33	Interleukin-33	2.79	.0986	–2.07	.1200	**5.76**	**.0302**	**8.88**	**.0153**	1.41	.3552	**6.28**	**.0007**
Mrc1	Mannose receptor C-type I	2.27	.2250	–1.88	.0941	4.27	.0717	4.11	.0704	1.02	.9455	**4.02**	**.0007**
Nos2	Inducible nitric oxide synthase 2	–1.43	.5301	–1.15	.8105	–1.24	.7760	1.43	.8898	3.19	.2560	–2.24	.3671
Osm	Oncostatin m	**4.75**	**.0021**	1.24	.4320	**3.83**	**.0027**	1.72	.1761	–1.61	.2597	**2.77**	**.0279**
Retnla	Resistin-like alpha	**40.36**	**.0092**	1.72	.1730	**23.41**	**.0191**	**149.41**	**.0004**	**1.70**	**.0264**	**88.06**	**<.0001**
Rorc	RAR-related orphan receptor C	1.04	.8217	–1.66	.4711	1.74	.4282	**–3.40**	**.0010**	1.13	.5665	–3.85	.1606
Socs1*	Suppressor of cytokine signaling 1	1.21	.6568	1.48	.2861	–1.22	.3177	1.32	.7036	–1.99	.5513	1.59	.2718
Socs3*	Suppressor of cytokine signaling 3	2.53	.1774	–1.32	.9220	3.34	.1820	**2.49**	**.0150**	–1.38	.2723	**3.42**	**.0015**
Socs5*	Suppressor of cytokine signaling 5	–1.10	.6731	–1.21	.7195	1.10	.9163	–1.73	.1751	–1.61	.2342	–1.08	.8446
Stat6*	Signal transducer and activator of transcription 6	–1.16	.8723	–1.13	.7899	–1.02	.9276	–1.81	.9638	1.01	.8856	–1.19	.9734
Tbx21*	T-box 21	–1.22	.1641	–1.61	.2801	1.32	.6222	**–4.81**	**.0499**	1.12	.6359	–5.41	.1558
Tlr2	Toll-like receptor 2	1.80	.0751	–1.54	.3681	2.77	.0508	1.17	.8601	1.14	.8165	1.03	.9483
Tlr4*	Toll-like receptor 4	1.22	.9522	–1.24	.5006	**1.51**	**.0212**	**2.25**	**.0261**	–1.06	.6651	**2.39**	**.0172**
Tlr6*	Toll-like receptor 6	–1.27	.5763	1.41	.7402	–1.79	.1521	1.39	.3729	–1.03	.7588	1.43	.2374
Tlr9	Toll-like receptor 9	1.07	.7891	–1.17	.0947	1.26	.4117	–1.32	.2012	–1.10	.8703	–1.21	.5235
Tslp	Thymic stromal lymphopoietin	–2.22	.2500	–1.23	.6110	–1.81	.397	**–8.76**	**.0030**	1.17	.7900	**–10.27**	**.0200**

Abbreviations: DC-SIGN, *Cd209a*; GATA, GATA binding protein 3; HIC, heat-inactivated conidia; MCP-3, monocyte-chemotactic protein 3; MINCLE, macrophage inducible calcium-dependent lectin receptor; mRNA, messenger RNA; RANTES, regulated on activation, normal T cell expressed and secreted.

NOTE. RT^2 Profiler PCR Array Mouse Th1 & Th2 responses. Unremarked genes represent additional data validated using TaqMan reverse transcriptase polymerase chain reaction method. Values in bold highlight significant up-regulation or down-regulation. The asterisk signifies which genes were measured using the RT2 Profiler PCR Array Mouse Th1 & Th2 response plates.

to normalize run-to-run variations.[13] The NSAF values were calculated as:

$$NSAF = (SpC/Mw)/\sum(SpC/Mw)\,n$$

where Mw is the molecular weight in kDa and n is the total number of proteins.

Statistical Analysis

Flow cytometry data were analyzed by measuring statistical differences between exposure groups by the test analysis of variance. Significance values are in comparison with air-exposed control animals at the same time point unless specifically noted. For the messenger RNA (mRNA) gene array results, the statistical analysis was performed using Qiagen's GeneGlobe Data Analysis Center. Genes with fold changes of 2 or less (down-regulated) or 2 or greater (up-regulated) were considered significantly altered. The *P* values were calculated based on a Student's *t*-test of the replicate values for each gene in the control and treatment groups, and *P* values ≤ .05 were considered significant. Proteomics data was compared by independent sample *t*-test for each protein in the exposure groups.

Results

Physical Characteristics, and Aerosolization of Viable and Heat-Inactivated Conidia (HIC)

Autoclaving viable *A fumigatus* resulted in significant reduction in conidial viability (99.81 ± 0.13 %) (Fig 1A) but did not alter

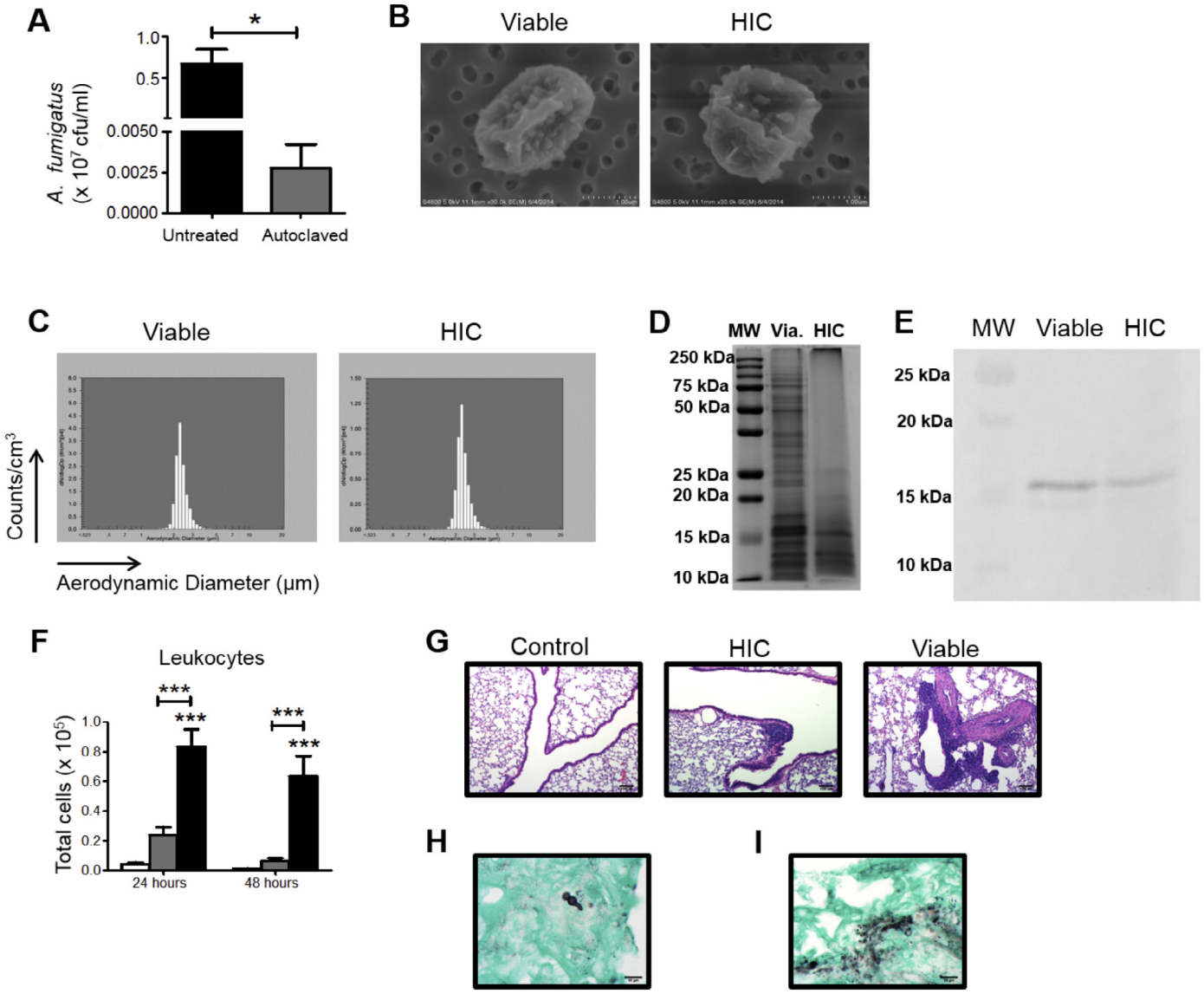

Figure 1. Morphological features, macromolecular composition, and pathological representation of HIC (heat-inactivated conidia) and viable *A fumigatus* conidia. (A) Graph representing impact of autoclaving on *A fumigatus* viability. Data represented as colony-forming units (cfu)/mL from 5 independent experiments. Black bar—Untreated *A fumigatus;* gray bar—autoclaved *A fumigatus.* (B) Representative scanning electron microscope (SEM) micrograph of aerosolized *A fumigatus* conidia deposited on polycarbonate filters. (C) Graph representing mean aerodynamic diameter of aerosolized *A fumigatus* conidia during exposures. (D) Sodium dodecyl sulfate polyacrylamide gel electrophoresis (SDS-PAGE) analysis of protein content of conidial extracts generated from HIC and viable *A fumigatus* conidia. MW, molecular weight marker; Via, viable conidia; HIC, heat-inactivated conidia. (E) Western blot analysis of conidial extracts of HIC and viable *A fumigatus* conidia. (F) Increased accumulation of leukocytes ($CD45^+$ cells) in murine airways caused by repeated inhalation of fungal conidia. Exposure groups: Control/naïve mice (white bars), HIC (gray bars), and viable conidia (black bars) (n = 8–10). (G) Hematoxylin and eosin–stained micrographs of murine lung tissues. Bar size = 100 µm. (H and I) Micrograph of Grocott's methenamine stain (GMS) sections of lung tissue from mice dosed with viable *A fumigatus* conidia. Bar size = 10 µm. For all graphs $^*P \le .05$, $^{***}P \le .001$.

conidial ornamentation because HIC retained the echinulate appearance of viable conidia (Fig 1B). The median aerodynamic diameter of the aerosolized conidia was also comparable (viable, 2.32 μm vs HIC, 2.31 μm) (Fig 1C). Heat inactivation of *A fumigatus* conidia resulted in degradation of high-molecular-weight proteins as visualized by SDS-PAGE (Fig 1D). Using sera developed previously,[8] we observed intact hydrophobins (~15 kDa) in conidial extracts derived from HIC and viable conidia (Fig 1E). Collectively, these data suggest that heat inactivation generates nonviable conidia that are incapable of germination yet retain broad structural features of intact conidia.

Repeated Dosing of B6C3F1/N Mice with Viable Conidia But Not HIC Results in Significant Inflammation and Airway Remodeling

Fungal viability did not influence overall health of animals because mice in all exposure groups gained weight at a similar rate through the course of the study. The BALF cell numbers were increased for both groups but were significantly elevated in animals inhaling viable conidia (Fig 1F). Histopathological assessment of lung tissue sections showed distinct inflammation for both exposure groups (Fig 1G). The blood vessels in lungs of mice inhaling viable conidia demonstrated significant remodeling as evidenced by thickening of arterial walls with polymorphonuclear cellular infiltration, whereas HIC exhibited unaffected vasculature (Fig 1G).

Lung tissue sections from mice stained with Grocott's Methenamine Silver (GMS) showed conidia in both groups. Conidia from HIC group did not exhibit any germination. In contrast, conidia with germ tubes were frequently observed in mice that were exposed to viable conidia (Fig 1H). Interestingly, fungal debris was noted within the thickened walls of the blood vessels (Fig 1I) and was restricted to mice exposed to viable conidia.

Fungal Viability Drives Eosinophilic Infiltration

Mice inhaling viable conidia exhibited a pleocellular infiltrate dominated by eosinophils (Fig 2). In contrast, eosinophils formed a minor population of leukocytes in airways of mice exposed to HIC. The transcripts for *Ccl11*, but not *Ccl5*, were significantly upregulated in murine lungs exposed to viable conidia (Table 1), suggesting that CCL11 likely plays an important role in selective recruitment of eosinophils in airways exposed to viable spores. Neutrophils were recruited at modest levels to airways of mice dosed with HIC compared with viable conidia.

Fungal Viability Influences the Phenotype of Innate Mediators

The impact of fungal viability on the phenotypic features of myelomonocytic cells was investigated. Alveolar macrophages (AMs) were gated as Siglec-F^{+}CD11c^{+} and autofluorescent^{hi} population[14] within the leukocyte fraction (gated CD45^{+} cells) and were significantly increased in airways of animals dosed with viable *A fumigatus* conidia (Fig 3A and 3B). A modest increase in AMs was noted in animals dosed with HIC but was smaller compared with the viable

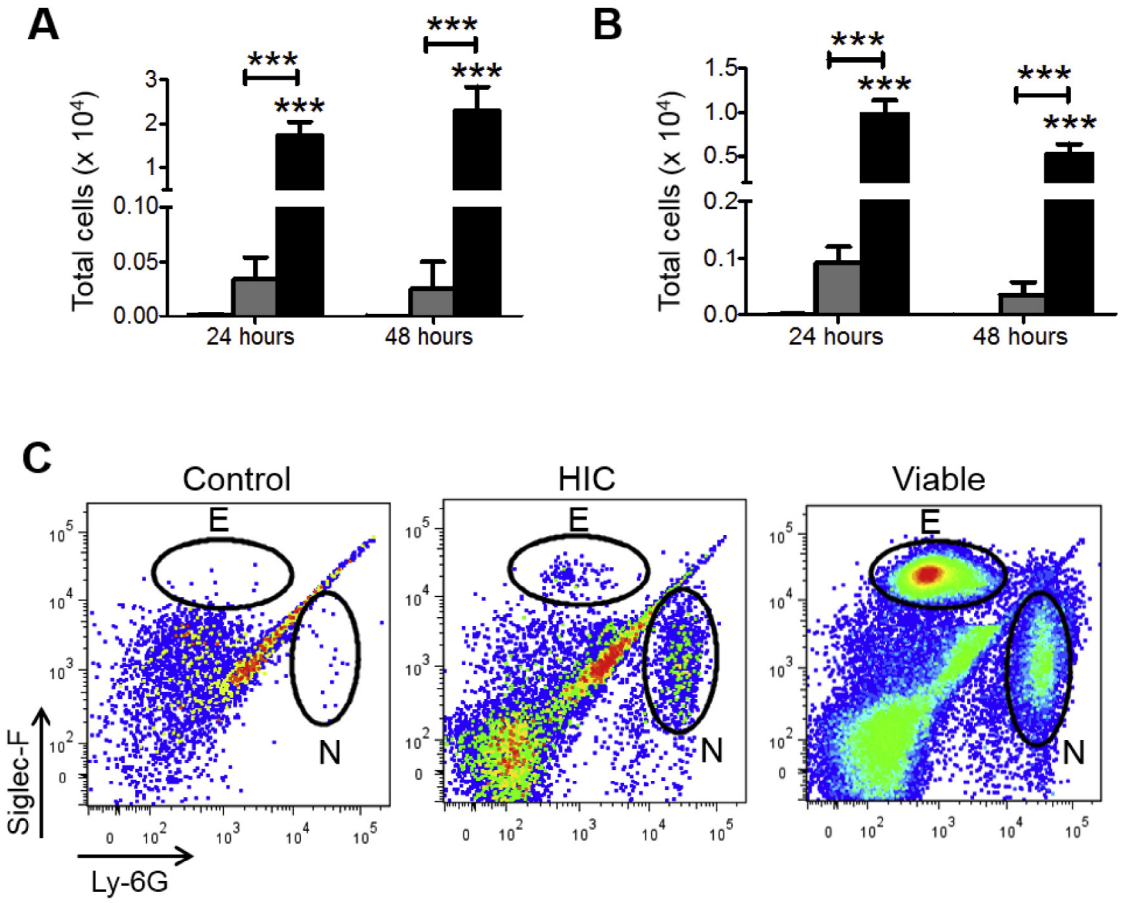

Figure 2. Recruitment of granulocytes to murine airways on inhalation of *A fumigatus* conidia. Total number of (A) eosinophils and (B) neutrophils in BALF samples (24 and 48 hours). (C) Dot plot representing distribution of eosinophils (SiglecF^{hi} Ly6G^{low}) and neutrophils (SiglecF^{low}Ly6G^{hi}) in BALF of mice inhaling HIC or viable *A fumigatus* conidia. E, eosinophils; N, neutrophils. For all graphs, ***$P \leq .001$ and exposure groups—control/naïve mice (white bars), HIC (gray bars), and viable conidia (black bars) (n = 8–10). BALF, bronchoalveolar lavage fluid; HIC, heat-inactivated conidia.

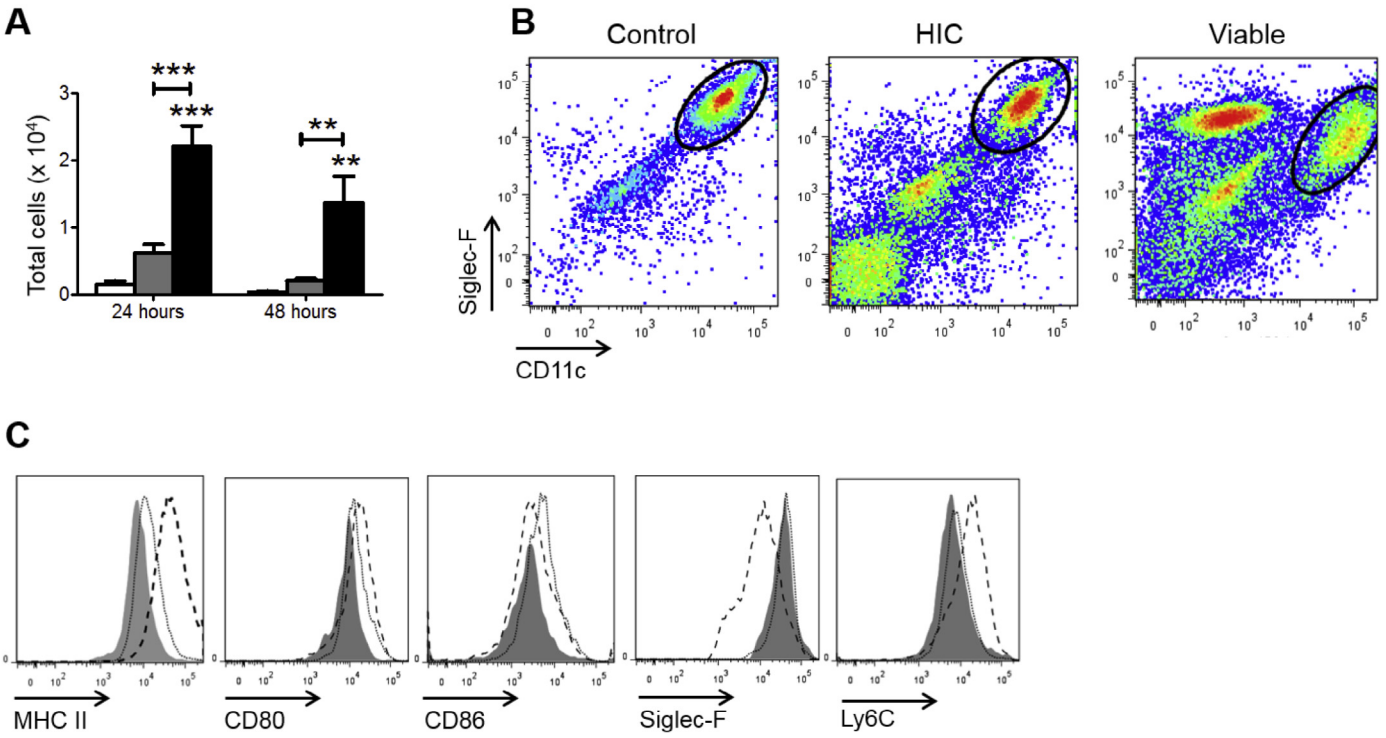

Figure 3. Distinct distribution and phenotype of alveolar macrophages (AMs) in response to HIC or viable *A fumigatus* conidia. (A) Total number of AMs in murine BALF after repeated inhalation of *A fumigatus* conidia. (B) Dot plot highlighting AM populations (SiglecF^{hi}CD11$c^{+/hi}$) in BALF samples. (C) Histograms displaying shifts in expression of various surface markers on gated AMs. Exposure groups—control/naïve mice (gray-shaded area), HIC (dotted line), and viable conidia (dashed line). For all graphs, $^{**}P \leq .01$; $^{***}P \leq .001$; and exposure groups—control/naïve mice (white bars), HIC (gray bars), and viable conidia (black bars) (n = 8–10). BALF, bronchoalveolar lavage fluid; HIC, heat-inactivated conidia.

group. To determine whether the increase in AMs was caused by local proliferation of resident cells or because of recruitment of monocytic precursors,[15,16] the expression of monocytic marker (Ly6C) on the AMs was examined. Ly6C expression was elevated on AMs exposed to viable conidia, indicating their recruitment from monocytes (Fig 3C). Surface expression of antigen presentation molecules was also evaluated on gated AMs to assess activation status (Fig 3C). Although expression of co-stimulatory molecules CD80 and CD86 were comparable in gated AMs from both fungal-exposed groups, major histocompatibility class (MHC) class II expression was significantly elevated in AMs from the viable conidia group. In the lungs of these mice, markers associated with M2 or alternatively activated macrophage (AAM) polarization (eg, *Arg1*, *Chil3,* and *Retnla*) were significantly up-regulated, whereas *Nos2* (M1 or classically activated macrophage marker) was down-regulated (Table 1). In contrast, mice dosed repeatedly with HIC-exposed mice showed no changes in expression of AAM polarization-associated markers. However, Nos2 expression increased in lungs of mice inhaling HIC.

Analysis of lung cell suspensions showed an increase in both CD103$^+$ DCs and CD11b^{hi} DCs (Fig 4A), although their MHC class II expression was not significantly altered (Fig 4B). No changes were noted in expression of co-stimulatory markers (CD80 and CD86). CD103$^+$ DCs have been shown to be critical for transporting antigens acquired in the airways to the lymph nodes and promoting allergic adaptive immune responses.[12] CD103$^+$ DCs accumulated in the mediastinal lymph nodes (MLNs) of mice from either group (Fig 4C). Although MHC class II expression was elevated, CD80 expression was decreased (Fig 4D). Expression of CD86 was marginally increased in CD103$^+$ DCs from the HIC group but remained unchanged in CD103$^+$ DCs from the viable group.

To characterize the fundamental differences of immune recognition of viable and HIC conidia, the expression of genes associated with various Toll-like receptors and C-type lectin receptors was investigated. Transcripts of *Tlr4* were elevated in lungs from the viable group, with no changes in expression of *Tlr2*, *Tlr6,* or *Tlr9*, whereas HIC remained unchanged or marginally decreased (Table 1). Among the C-type lectin receptors, a significant up-regulation of *Mrc1* gene (encoding the mannose receptor) was observed in the lungs of mice exposed to viable conidia, but not HIC. Dectin-1 encoded by *Clec7a* recognizes fungal β-1,3/β-1,6-linked glucans on the surface of germinating spores. As expected, lungs from mice exposed to viable conidia showed significantly higher levels of *Clec7a* transcripts compared with HIC. No differences were noted between viable and HIC conidia in the expression of *Clec4e*, MINCLE, *Clec4n* (Dectin-2), *Cd163* (scavenger receptor), and *Cd209a* (DC-SIGN) transcripts between the viable and HIC groups.

Fungal Viability Drives Differential Antifungal Adaptive Immune Responses

The BALF cells were activated in vitro, stained for specific cytokines, and analyzed by flow cytometry to characterize the nature of adaptive immune responses. The number of CD4$^+$ T lymphocytes accumulating in airways was comparable between exposure groups at 24 hours, whereas at 48 hours a significant difference was observed (Fig 5A). The total number of CD8$^+$ T cells also increased with viable conidia. At 24 hours, higher numbers of interferon gamma (IFN-γ)$^+$ subpopulations were observed in airways of mice from HIC group (Fig 5B). A reverse trend in IFN-γ$^+$ subpopulations of CD4$^+$ T cells was observed at 48 hours. Nevertheless, the expression of IFN-γ continued to be significantly higher in CD4$^+$ T cells from the HIC group as determined by mean fluorescence intensity (MFI) for IFN-γ on gated CD4$^+$ T cells (Fig 5B). Mice exposed to viable conidia were also dominated by CD8$^+$ T cells expressing IFN-γ (T_C1)

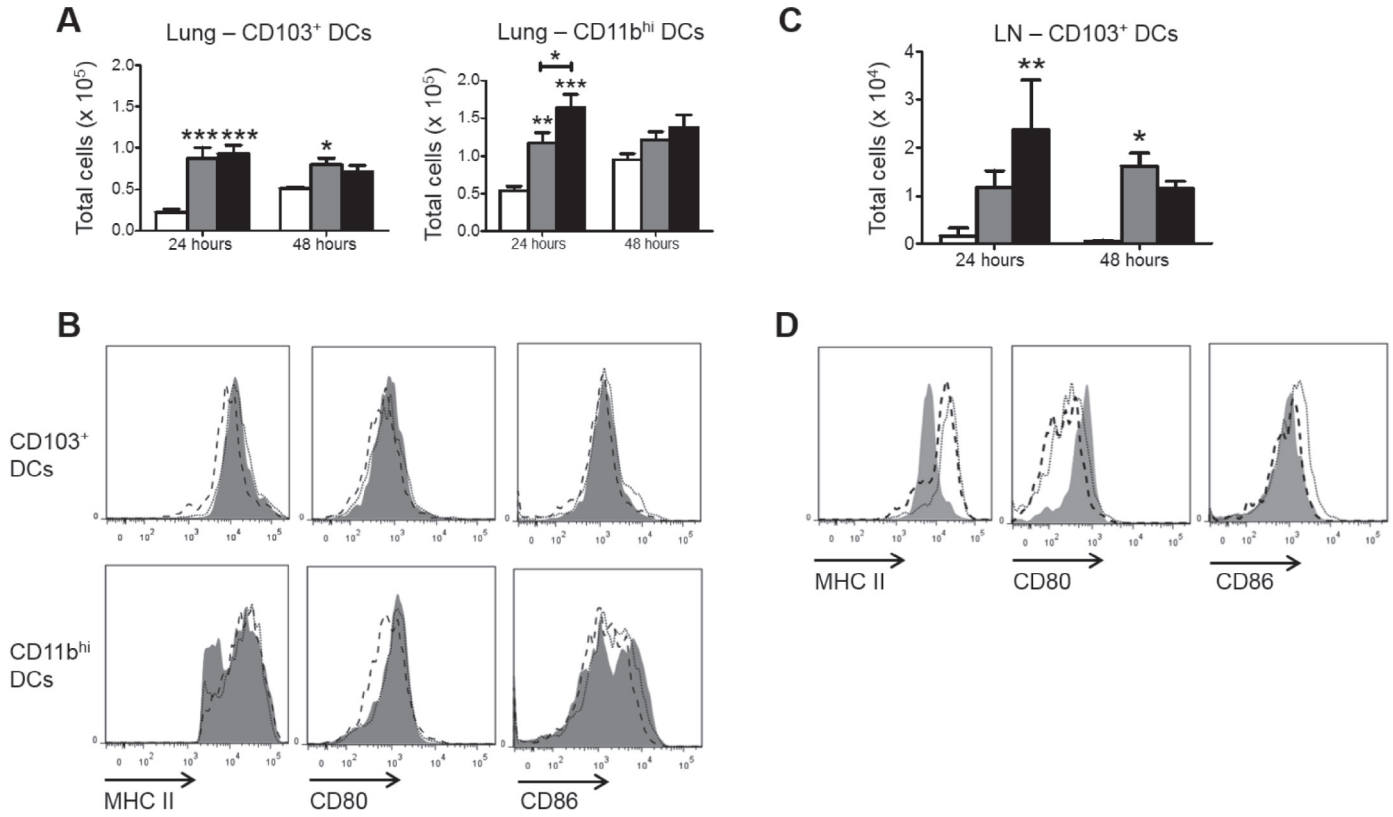

Figure 4. Distribution of dendritic cell (DC) subpopulations after exposure to HIC or viable *A fumigatus* conidia. (A) Total cell numbers of $CD103^+$ DCs and $CD11b^{hi}$ DCs in lung tissue after BALF removal. (B) Histograms displaying shifts in expression of markers associated with antigen presentation on DC subpopulations. Exposure groups—control/naïve mice (gray-shaded area), HIC (dotted line), and viable conidia (dashed line). (C) Accumulation of $CD103^+$ DCs in the mediastinal lymph nodes (MLNs). (D) Histograms displaying shifts in expression of markers associated with antigen presentation on gated $CD103^+$ DCs. Exposure groups—control/naïve mice (gray-shaded area), HIC (dotted line), and viable conidia (dashed line). For all graphs, $^*P \leq .05$; $^{**}P \leq .01$; $^{***}P \leq .001$; and exposure groups—control/naïve mice (white bars), HIC (gray bars), and viable conidia (black bars) (n = 8–10). BALF, bronchoalveolar lavage fluid; HIC, heat-inactivated conidia.

(Fig 5C). Interleukin-$17A^+$ $CD8^+$ T cells (T_C17) were also frequently identified in mice from the viable group but formed a small population in comparison with T_C1 cells. Very low numbers of T_C17 and T_C1 populations were observed in response to HIC.

Fungal Germination is Critical for the Development of Allergic Airway Inflammation

Periodic acid-Schiff staining of lung tissue sections demonstrated goblet cell metaplasia in mice dosed with viable conidia (Fig 6A), whereas mice exposed to HIC showed no similar features. $CD4^+$ T cells expressing IL-13 were significantly increased in total cell number and MFI on exposure to viable conidia (Fig 6B). Interleukin-5–expressing $CD4^+$ T cells formed a minor population in both viable and HIC exposures (Fig 6B). A fraction of IFN-γ^+ (T_H1) and IL-$17A^+$ (T_H17) expressing $CD4^+$ T cells (~30%) also co-expressed the pro-allergic cytokine, IL-13 (Fig 6C). Analysis of MFI for this T cell subpopulation showed higher expression of IL-13 in the viable group. We also noted that *Gata3*, the transcription factor associated with T_H2 cell differentiation, was either down-regulated or remained unchanged (Table 1) in the viable conidia group.

Recent studies have shown that epithelial cells play an active role in allergic outcomes through expression of IL-33, IL-25, and thymic stromal lymphopoietin, so we assessed expression of these genes in our study.[17] Messenger RNA expression analysis revealed up-regulation of *Il33* and *Il1rl1*, which encode for IL-33 and its receptor (ST2), respectively, in lungs of mice exposed specifically to viable *A fumigatus* conidia (Table 1). Transcripts for other epithelial cytokines were either not detected or were down-regulated at the evaluated time points.

Analysis of BALF samples also showed accumulation of B lymphocytes in the airways of mice inhaling viable conidia (Fig 7A). Repeated exposure to viable or HIC conidia stimulated B cells in the MLNs of mice; with higher total number of B cells in response to viable conidia (Fig 7A). Serum concentrations of the allergy-associated immunoglobulins (IgG_1 and IgE) were significantly elevated in mice that inhaled viable conidia when compared with both air control and the HIC group (Fig 7B).

Mitochondrial Dysregulation

Proteomic analysis of whole lung showed alterations in abundance of proteins associated with broader metabolic activities in lungs (eFigure 1). Chitinase-like proteins 3 and 4, which are expressed in an IL-13–dependent manner, were more abundant in mice inhaling viable conidia. Other pro-allergic proteins associated with asthma phenotype included peptidyl-prolyl cis-trans isomerases, prostaglandin E synthase 3, and protein S100-A9. Down-regulation of proteins involved in the maintenance of extracellular matrix and intercellular adhesive contacts (eg, integrin-linked protein kinase and gamma-adducin) were indicative of disruption of epithelial integrity in lung tissue.

Repeated inhalation of *A fumigatus* also increased the abundance of antimicrobial proteins, eg, neutrophil gelatinase-associated lipocalin, surfactant-protein D in lungs of mice. Furthermore, proteomics showed increased abundance of novel markers (eg,

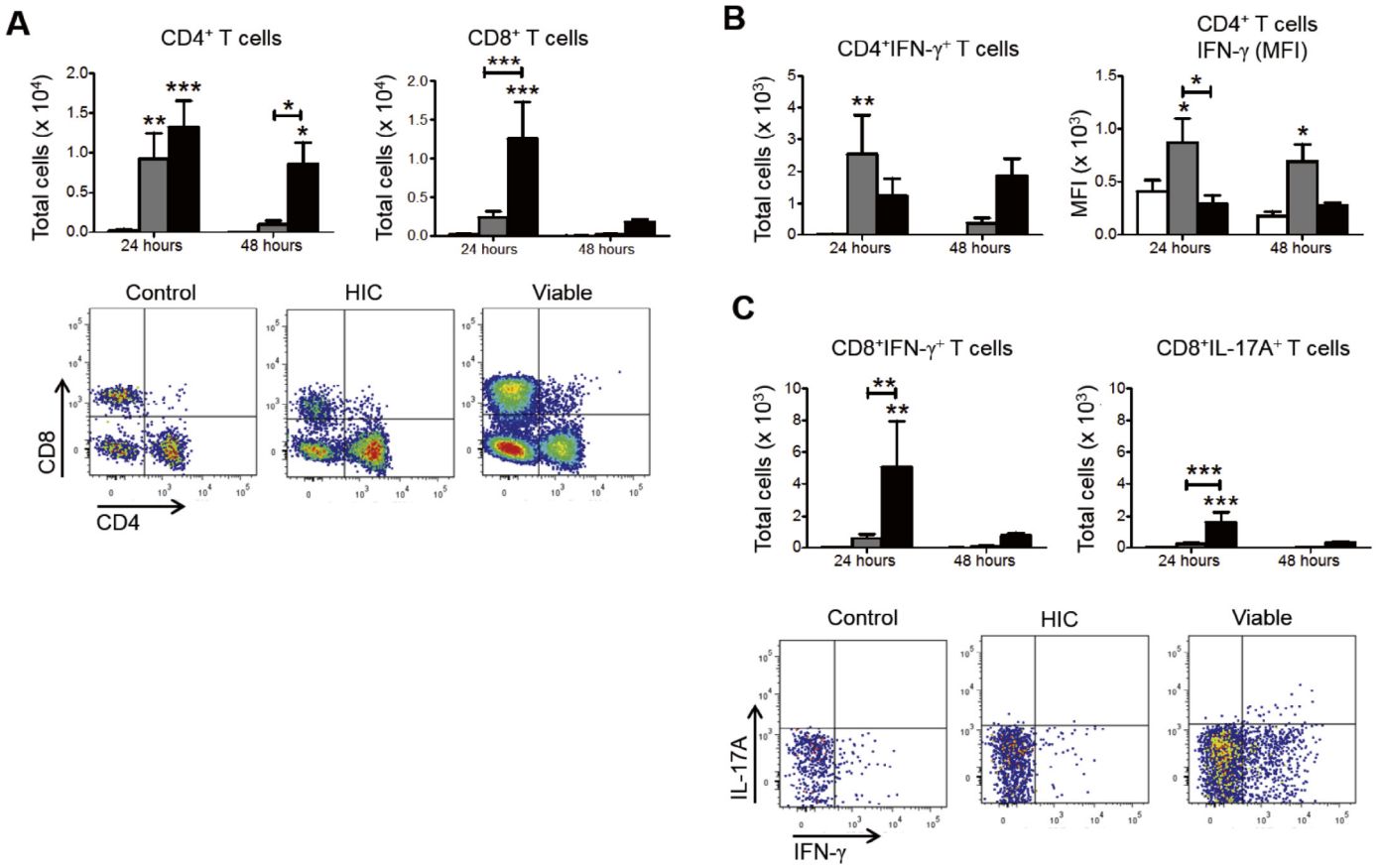

Figure 5. Development of antifungal adaptive immune responses during chronic exposure to *A fumigatus* conidia. (A) Distribution of $CD4^+$ and $CD8^+$ T cells in the airways of mice at 24 and 48 hours after repeated dosing with HIC or viable conidia for 13 weeks. (B) Total number of IFN-γ expressing $CD4^+$ T cells infiltrating the airways and mean fluorescence intensity (MFI) for IFN-γ in $CD4^+$ T cells. (C) Total cell numbers and dot plots of IFN-γ and IL-17A expressing $CD8^+$ T cells in the airways. For all graphs, $^*P \leq .05$; $^{**}P \leq .01$; $^{***}P \leq .001$ and exposure groups—Control/naïve mice (white bars), HIC (gray bars), and viable conidia (black bars) (n = 8–10). HIC, heat-inactivated conidia; IFN-γ, interferon gamma.

galectin-3, prosaposin) with poorly defined roles in allergic airway inflammation.

Quantitative proteomics of lung tissue also indicated significant mitochondrial dysregulation because proteins associated with this organelle were significantly down-regulated, with approximately 35% of the total proteins that were in lower abundance in mice exposed to viable *A fumigatus*. Ingenuity Pathway Analysis (http://www.ingenuity.com, IPA; Qiagen, Redwood City, California) showed that most down-regulated proteins are associated with complex III within the mitochondrial electron transport chain system (eFigure 2). These changes extended to other membrane-bound organelles such as the endoplasmic reticulum (ER), as evidenced by significantly altered abundance of major proteins associated with ER function.

Discussion

A fumigatus conidia are typically metabolically inactive, but they are capable of growth after favorable environmental cues. Exposure to these collective variables typically results in germination and release of enzymes and secondary metabolites that promote the breakdown of organic substrates. Germinating *A fumigatus* secrete proteases that mediate immune responses toward a Th2 phenotype. Our study provides evidence that *A fumigatus* viability within the host is essential for development of allergic inflammation in mice, driving distinct composition of inflammation and histopathological presentations. The capacity of *A fumigatus* to germinate in vivo directs allergic inflammation and is highlighted by goblet cell metaplasia, eosinophilia, expansion of $CD4^+$ T cells expressing IL-13, along with increased serum IgE and up-regulation of mediators of allergic inflammation, thus providing mechanistic insight into the fundamental recognition of viable conidia by immune cells.

Our data suggest that subchronic pulmonary exposure to viable *A fumigatus* conidia may result in polarization of resident macrophages into AAMs, which are implicated in allergic diseases.[18] This finding is supported by up-regulation of *Arg1*, *Chil3,* and *Retnla*, and down-regulation of *iNos* in lung tissue. Furthermore, expression of *Mrc1* and *Clec7a* also increased in lungs of mice that inhaled viable conidia. The *Mrc1* gene encodes for mannose receptor, a lectin that recognizes mannose residues, and *Clec7a* encodes for dectin-1, a receptor of β-glucan that is specifically expressed during germination but not in dormant or heat-inactivated *A fumigatus* conidia.[19] This is additionally supported by our observation in GMS-stained lung tissue sections, where biologically active germinating conidia were observed only in the viable group. *Mrc1* was the first characterized marker of AAMs.[20,21] *Clec7a* is also suggested to be up-regulated in AAMs.[22] Finally, in the presence of IL-13, increased IL-33 can amplify the polarization of AAMs via ST2.[23,24] The polarization of alveolar macrophages in response to viable, but not HIC, is likely driven by an influx of inflammatory monocytes to the site of inflammation as previously shown.[25,26] Quantitative proteomics showed increased abundance of ankycorbin and galectin-3, which promote differentiation of inflammatory monocytes into AAMs.[27,28] The AAMs are formed after acute exposure to *A fumigatus*,[29] and persistence

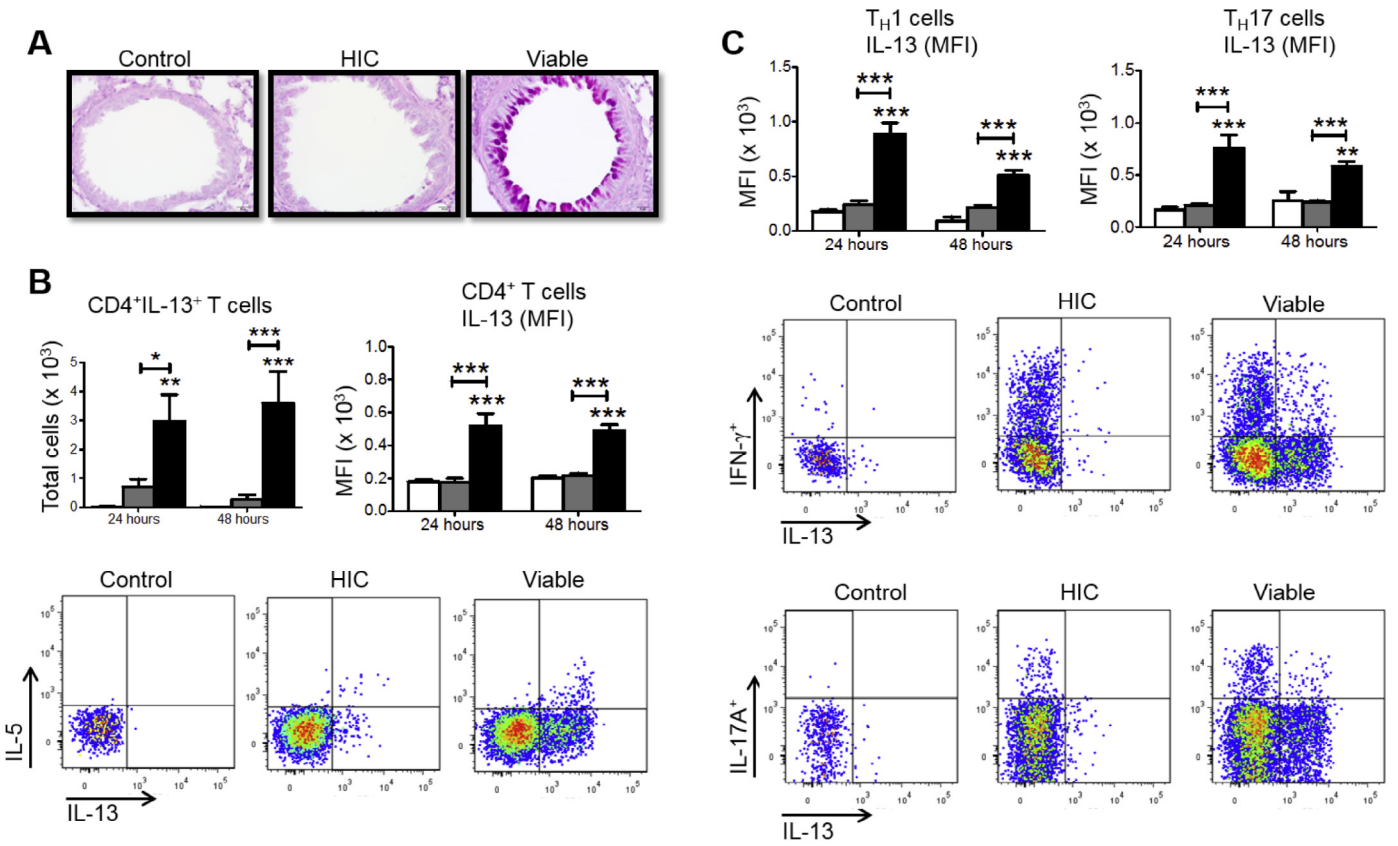

Figure 6. Contrasting representation of allergic disease in lungs of mice inhaling HIC or viable *A fumigatus* conidia. (A) Alcian blue–periodic acid-Schiff staining of paraffin-embedded mouse lung tissue sections. Bar size = 20 μm. (B) Total cell numbers and dot plot representation of IL-13$^+$ and IL-5$^+$ CD4$^+$ T cells in the airways. (C) MFI (IL-13 expression) of IL-13$^+$ T_H1 and T_H17 cells in the airways. For all graphs, *$P \leq .05$; **$P \leq .01$; ***$P \leq .001$; and exposure groups—Control/naïve mice (white bars), HIC (gray bars), and viable conidia (black bars) (n = 8–10). HIC, heat-inactivated conidia; IL, interleukin; MFI, mean fluorescence intensity.

of AAMs in the airways of mice exposed to viable conidia may functionally impact airway disease, because AAMs are less efficient in killing phagocytosed microbes.[30,31] Our observations suggest that fungal viability may influence AM polarization; however, the formation of AMs well after embryogenesis is controversial, and the population observed in our studies may represent exudative macrophages previously described.[32] Finally, the markers discussed here are expressed in other cell types, including epithelial cells.

Previously, viability of *A fumigatus* conidia has been reported to influence the recruitment and differentiation of the responding immune cells.[3,4] Formation of IFN-γ expressing CD4$^+$ T cell subpopulations is restricted to mice instilled with viable *A fumigatus,* and heat-inactivation promoted T_H2 responses.[3] Similarly, we demonstrated that IFN-γ$^+$CD4$^+$ T cells were formed preferentially after instillation of viable conidia, and eosinophils were significantly higher in airways of mice exposed to HIC.[4] However, in our revised aerosol exposure, we observed that the viability of inhaled conidia has a distinct outcome. We now demonstrate that following repeated exposure of HIC, IFN-γ–expressing CD4$^+$ T cells migrate to the airways with overall numbers comparable to those of mice inhaling viable spores. Furthermore, this subpopulation of CD4$^+$ T cells from HIC express more IFN-γ on a per-cell basis. Our studies showed that some IL-13$^+$CD4$^+$ T cells are recruited to the airways after HIC administration. Similarly, expression of IL-13 on a per-cell basis also increased. Because heat inactivation was the primary method of generating HIC in both studies, one could hypothesize that the total number of conidia administered or the differences in the dosing methods (instillation vs inhalation) may explain the discordance. The AGS system allows for the administration of unmodified conidia, whereas instillation relies on delivery of conidial suspension using a fluid that may release surface carbohydrates and glycoproteins in the solution, thus altering conidial surface and downstream immunological recognition.

A puzzling observation in our studies is the detection of CD4 T cells (T_H) that exhibit bi-functionality by co-expressing pro-allergic cytokine IL-13 and the pro-inflammatory cytokines IFN-γ or IL-17A. Transcription factors for lineage-commitment (*Gata3, Rorc, Tbx21*) of T_H cells were either down-regulated or remained unchanged in the lungs. Based on the repeated nature of the antigenic stimulus, possibly memory T cells are formed in our model; however, memory T_H2 cells cannot maintain T_H2 cytokine profile during down-regulation of *Gata3* expression.[33] CD4 memory T cells that are uncommitted to a particular lineage have been reported.[34] Alternatively, the T cells observed in our study could be naïve T cells that are stimulated to release multiple cytokines. Epithelial IL-33 can bind to the ST2 receptor expressed on naïve T cells and stimulate them to release IL-13.[35] Additional studies are required to resolve the identity of T cells formed in response to repeated inhalation of fungi.

Uptake of viable *A fumigatus* conidia by innate immune cells results in the up-regulation of specific receptors, such as dectin-1, which mediate production of reactive oxygen species (ROS) by mitochondria and are essential for antimicrobial function.[36,37] If unquenched, mitochondrial ROS is cytotoxic to host cells. Quantitative proteomics and IPA showed that repeated exposure to viable *A fumigatus* resulted in altered expression of proteins indicative of mitochondrial dysfunction and ER stress. Recently, mitochondrial dysfunction and ER stress have been associated with allergic asthma.[38–40] Excess ROS production from repeated microbial

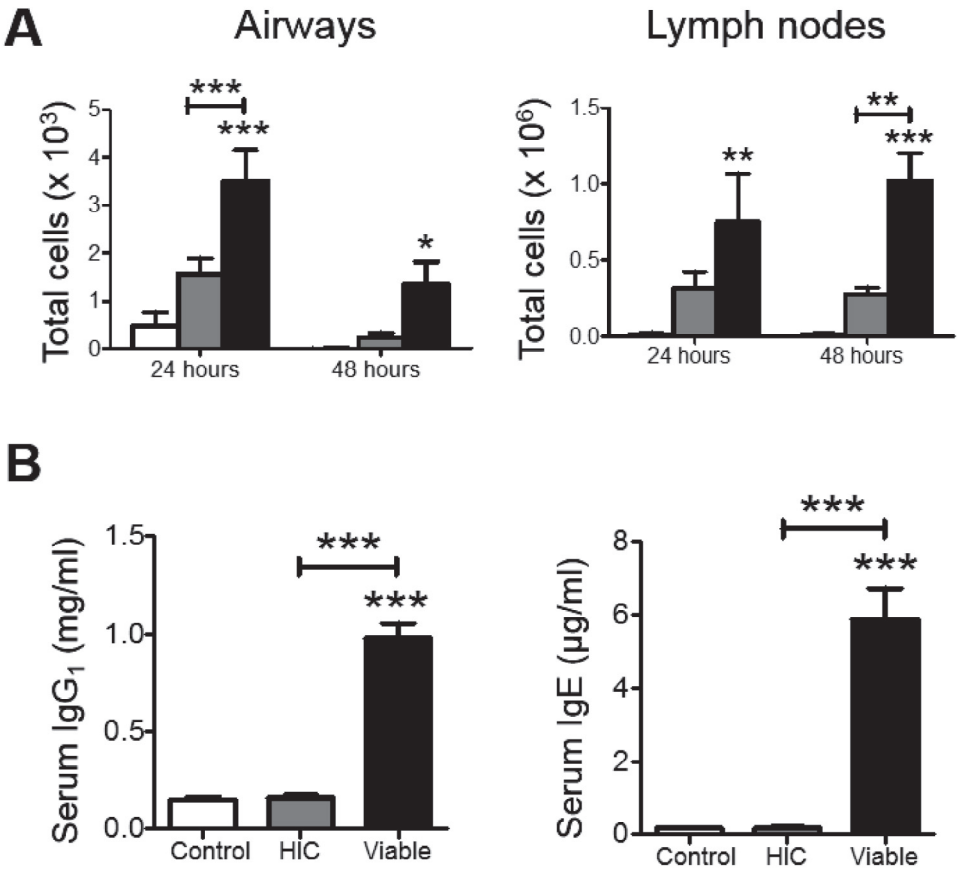

Figure 7. Development of B cell responses to inhaled conidia and characterization of antibody responses. (A) Recruitment of B cells (CD19+) in the airways and expansion in the MLNs. (B) Mouse serum concentration of total IgG1 and IgE as determined by ELISA. For all graphs, *P ≤ .05, **P ≤ .01; ***P ≤ 0.001; and exposure groups—Control/naïve mice (white bars), HIC (gray bars), and viable conidia (black bars) (n = 8–10). ELISA, enzyme-linked immunosorbent assay; HIC, heat-inactivated conidia; Ig, immunoglobulin; MLN, mediastinal lymph node.

exposure could potentially contribute to oxidative stress-induced organelle dysfunction. However, whether the altered expression of proteins associated with organelles is pathognomonic or a normal response in our model is unclear.

Collectively, the results suggest that the viability of inhaled *A fumigatus* conidia shapes the immunological outcomes. Specifically, repeated exposure to viable *A fumigatus* drives allergic inflammation and may render the host pulmonary system to a potential constant state of repeated oxidative stress, influencing the metabolic functioning of cell organelles. The results of this study suggest that strategies restricting fungal germination and reversing the oxidative damage may be useful in limiting allergic inflammation, providing new avenues for therapeutics.

Acknowledgments

The authors thank Amy Cumpston, Jared Cumpston, Walter McKinney, and Howard Leonard for conducting animal exposures, Brandon F. Law for assistance in animal procedures, Diane Schwegler-Berry for assistance with electron microscopy, and Dr. Marlene Orandle for interpretation of histopathology. The findings and the conclusions in this report are those of the authors and do not necessarily represent the views of the National Institute for Occupational Safety and Health (NIOSH).

Supplementary Data

Supplementary data related to this article can be found at https://doi.org/10.1016/j.anai.2018.04.008.

References

[1] Segal BH. Aspergillosis. *N Engl J Med*. 2009;360:1870–1884.
[2] Eduard W. Fungal spores: a critical review of the toxicological and epidemiological evidence as a basis for occupational exposure limit setting. *Crit Rev Toxicol*. 2009;39:799–864.
[3] Rivera A, Van Epps HL, Hohl TM, Rizzuto G, Pamer EG. Distinct CD4+-T-cell responses to live and heat-inactivated *Aspergillus fumigatus* conidia. *Infect Immun*. 2005;73:7170–7179.
[4] Templeton SP, Buskirk AD, Law B, Green BJ, Beezhold DH. Role of germination in murine airway CD8+ T-cell responses to *Aspergillus* conidia. *PLoS ONE*. 2011;6:e18777.
[5] Horner WE, Helbling A, Salvaggio JE, Lehrer SB. Fungal allergens. *Clin Microbiol Rev*. 1995;8:161–179.
[6] Green BJ, Mitakakis TZ, Tovey ER. Allergen detection from 11 fungal species before and after germination. *J Allergy Clin Immunol*. 2003;111:285–289.
[7] Tomee JF, Kauffman HF. Putative virulence factors of *Aspergillus fumigatus*. *Clin Exp Allergy*. 2000;30:476–484.
[8] Buskirk AD, Green BJ, Lemons AR, et al. A murine inhalation model to characterize pulmonary exposure to dry Aspergillus fumigatus conidia. *PLoS ONE*. 2014;9:e109855.
[9] Buskirk AD, Templeton SP, Nayak AP, et al. Pulmonary immune responses to Aspergillus fumigatus in an immunocompetent mouse model of repeated exposures. *J Immunotoxicol*. 2014;11:180–189.
[10] Nayak AP, Green BJ, Lemons AR, et al. Subchronic exposures to fungal bioaerosols promotes allergic pulmonary inflammation in naive mice. *Clin Exp Allergy*. 2016;46:861–870.
[11] Croston TL, Nayak AP, Lemons AR, et al. Influence of Aspergillus fumigatus conidia viability on murine pulmonary microRNA and mRNA expression following subchronic inhalation exposure. *Clin Exp Allergy*. 2016;46:1315–1327.
[12] Nakano H, Free ME, Whitehead GS, et al. Pulmonary CD103+ dendritic cells prime Th2 responses to inhaled allergens. *Mucosal Immunol*. 2012;5:53–65.
[13] Zybailov B, Mosley AL, Sardiu ME, Coleman MK, Florens L, Washburn MP. Statistical analysis of membrane proteome expression changes in Saccharomyces cerevisiae. *J Proteome Res*. 2006;5:2339–2347.

[14] Misharin AV, Morales-Nebreda L, Mutlu GM, Budinger GR, Perlman H. Flow cytometric analysis of macrophages and dendritic cell subsets in the mouse lung. *Am J Respir Cell Mol Biol*. 2013;49:503–510.
[15] Stumm CL, Wettlaufer SH, Jancar S, Peters-Golden M. Airway remodeling in murine asthma correlates with a defect in PGE2 synthesis by lung fibroblasts. *Am J Physiol Lung Cell Mol Physiol*. 2011;301:L636–L644.
[16] Gordon S, Taylor PR. Monocyte and macrophage heterogeneity. *Nat Rev Immunol*. 2005;5:953–964.
[17] Divekar R, Kita H. Recent advances in epithelium-derived cytokines (IL-33, IL-25, and thymic stromal lymphopoietin) and allergic inflammation. *Curr Opin Allergy Clin Immunol*. 2015;15:98–103.
[18] Gordon S. Alternative activation of macrophages. *Nat Rev Immunol*. 2003;3:23–35.
[19] Hohl TM, Van Epps HL, Rivera A, et al. *Aspergillus fumigatus* triggers inflammatory responses by stage-specific b-glucan display. *PLoS Pathog*. 2005;1:e30.
[20] Stein M, Keshav S, Harris N, Gordon S. Interleukin 4 potently enhances murine macrophage mannose receptor activity: a marker of alternative immunologic macrophage activation. *J Exp Med*. 1992;176:287–292.
[21] Gundra UM, Girgis NM, Ruckerl D, et al. Alternatively activated macrophages derived from monocytes and tissue macrophages are phenotypically and functionally distinct. *Blood*. 2014;123:e110–e122.
[22] Willment JA, Lin HH, Reid DM, et al. Dectin-1 expression and function are enhanced on alternatively activated and GM-CSF-treated macrophages and are negatively regulated by IL-10, dexamethasone, and lipopolysaccharide. *J Immunol*. 2003;171:4569–4573.
[23] Kurowska-Stolarska M, Stolarski B, Kewin P, et al. IL-33 amplifies the polarization of alternatively activated macrophages that contribute to airway inflammation. *J Immunol*. 2009;183:6469–6477.
[24] Li D, Guabiraba R, Besnard AG, et al. IL-33 promotes ST2-dependent lung fibrosis by the induction of alternatively activated macrophages and innate lymphoid cells in mice. *J Allergy Clin Immunol*. 2014;134:1422–1432.
[25] Girgis NM, Gundra UM, Ward LN, Cabrera M, Frevert U, Loke P. Ly6C^{high} monocytes become alternatively activated macrophages in schistosome granulomas with help from CD4^{+} cells. *PLoS Pathog*. 2014;10:e1004080.
[26] Espinosa V, Jhingran A, Dutta O, et al. Inflammatory monocytes orchestrate innate antifungal immunity in the lung. *PLoS Pathog*. 2014;10:e1003940.
[27] MacKinnon AC, Farnworth SL, Hodkinson PS, et al. Regulation of alternative macrophage activation by galectin-3. *J Immunol*. 2008;180:2650–2658.
[28] Sordet O, Rebe C, Plenchette S, et al. Specific involvement of caspases in the differentiation of monocytes into macrophages. *Blood*. 2002;100:4446–4453.
[29] Bhatia S, Fei M, Yarlagadda M, et al. Rapid host defense against *Aspergillus fumigatus* involves alveolar macrophages with a predominance of alternatively activated phenotype. *PLoS ONE*. 2011;6:e15943.
[30] Xavier MN, Winter MG, Spees AM, et al. PPARg-mediated increase in glucose availability sustains chronic *Brucella abortus* infection in alternatively activated macrophages. *Cell Host Microbe*. 2013;14:159–170.
[31] Eisele NA, Ruby T, Jacobson A, et al. *Salmonella* require the fatty acid regulator PPARdelta for the establishment of a metabolic environment essential for long-term persistence. *Cell Host Microbe*. 2013;14:171–182.
[32] Osterholzer JJ, Chen GH, Olszewski MA, et al. Chemokine receptor 2-mediated accumulation of fungicidal exudate macrophages in mice that clear cryptococcal lung infection. *Am J Pathol*. 2011;178:198–211.
[33] Endo Y, Hirahara K, Yagi R, Tumes DJ, Nakayama T. Pathogenic memory type Th2 cells in allergic inflammation. *Trends Immunol*. 2014;35:69–78.
[34] Youngblood B, Hale JS, Ahmed R. T-cell memory differentiation: insights from transcriptional signatures and epigenetics. *Immunology*. 2013;139:277–284.
[35] Kakkar R, Lee RT. The IL-33/ST2 pathway: therapeutic target and novel biomarker. *Nat Rev Drug Discov*. 2008;7:827–840.
[36] Gantner BN, Simmons RM, Canavera SJ, Akira S, Underhill DM. Collaborative induction of inflammatory responses by dectin-1 and Toll-like receptor 2. *J Exp Med*. 2003;197:1107–1117.
[37] Gantner BN, Simmons RM, Underhill DM. Dectin-1 mediates macrophage recognition of Candida albicans yeast but not filaments. *EMBO J*. 2005;24:1277–1286.
[38] Mabalirajan U, Dinda AK, Kumar S, et al. Mitochondrial structural changes and dysfunction are associated with experimental allergic asthma. *J Immunol*. 2008;181:3540–3548.
[39] Wiegman CH, Michaeloudes C, Haji G, et al. Oxidative stress-induced mitochondrial dysfunction drives inflammation and airway smooth muscle remodeling in patients with chronic obstructive pulmonary disease. *J Allergy Clin Immunol*. 2015;136:769–780.
[40] Aguilera-Aguirre L, Bacsi A, Saavedra-Molina A, Kurosky A, Sur S, Boldogh I. Mitochondrial dysfunction increases allergic airway inflammation. *J Immunol*. 2009;183:5379–5387.

Supplementary Data

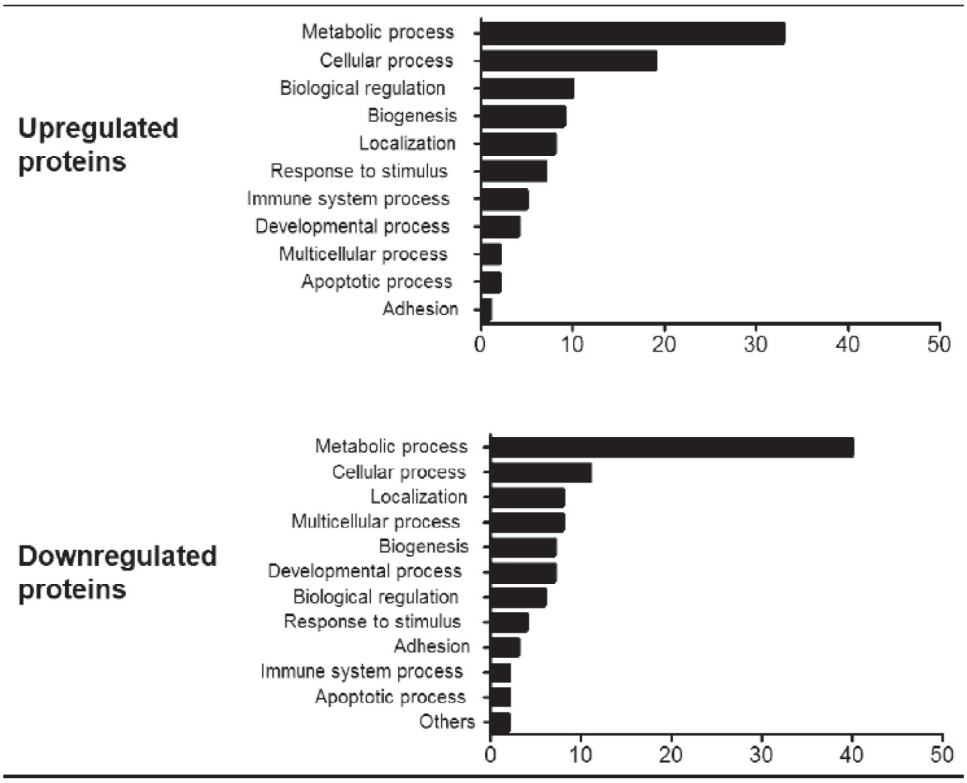

eFigure 1. Gene ontology (GO) Biological process of altered expression of proteins in murine lung tissue. Data reflects % proteins with altered expression associated with each biological process.

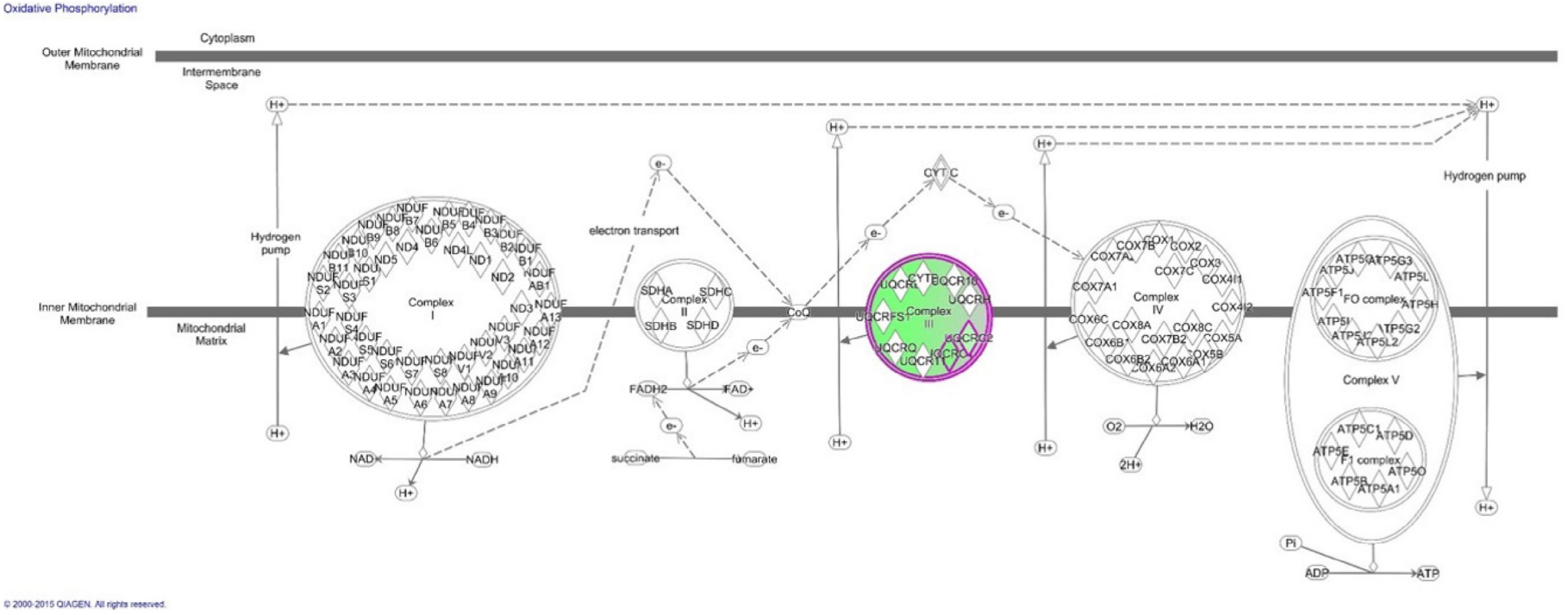

eFigure 2. Distribution of mitochondrial proteins with altered expression profile. Ingenuity pathway analysis (IPA) indicating association of proteins with altered expression to the Complex III of the mitochondrial electron transport chain.